

Design, Synthesis, and Microbiological Evaluation of New *Candida albicans* CYP51 Inhibitors

Fausto Schiaffella,[†] Antonio Macchiarulo,[†] Lara Milanese,[†] Anna Vecchiarelli,[‡] Gabriele Costantino,[†] Donatella Pietrella,[‡] and Renata Fringuelli^{*,†}

Department of Drug Chemistry and Technology and Department of Experimental Medicine and Biochemical Sciences, University of Perugia, Perugia, Italy

Received July 19, 2005

In a program aimed at the design and synthesis of novel azole inhibitors of *Candida albicans* CYP51 (CA-CYP51), a series of azole 1,4-benzothiazines (BT) and 1,4-benzoxazines (BO) were recently synthesized. A morphological study of the enzyme active site highlighted a hydrophobic access channel, and a docking study pointed out that the C-2 position of the BT or BO nucleus was oriented toward the access channel. Here, we report the design, synthesis, and microbiological evaluation of C-2-alkyl BT and BO compounds. In both series, introduction of the alkyl chain maintained and in some cases improved the anti-*Candida* in vitro activity; however, there was not always a strict correlation between in vitro and in vivo activity for several compounds.

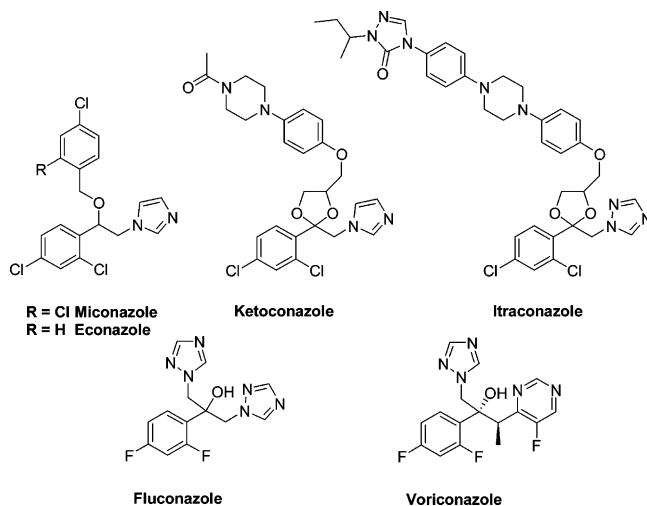
Introduction

In recent years, fungal infections have increased markedly and one of the main agents is the opportunistic pathogen *Candida albicans*. A major obstacle in the treatment of *C. albicans* infections is the spread of antifungal drug resistance mainly in patients chronically subjected to antimycotic therapy, i.e., those treated with broad-spectrum antibiotics, immunosuppressive agents, anticancer, and anti-AIDS drugs.^{1,2}

Azole and non-azole antifungal agents are usually used to treat *Candida* infections, but despite the good antifungal activities observed in vitro, candidemia is still a major cause of death.¹ Many valid therapy programs fail because of widespread secondary *C. albicans* infections. New effective anti-*Candida* agents are needed to combat the drug-resistant strains and widespread diffusion of *C. albicans*.

Up to only 30 years ago, the choice of systemically available antimycotics was almost exclusively amphotericin B with all of its adverse side effects. Then a series of inhibitors of the biosynthesis of ergosterol, the major sterol of the fungal cell membrane, were found that had excellent antifungal activity and were safer; some were also active after oral or parenteral application.³ Starting with miconazole and ketoconazole, and improved with fluconazole, itraconazole, and voriconazole, the azoles have been a mainstay of the antifungal armamentarium (Chart 1). These drugs inhibit the synthesis of ergosterol by binding to the heme cofactor located in the active site of the P450-dependent enzyme lanosterol 14 α -demethylase (CYP51). It has been proposed that ergosterol depletion, coupled with the accumulation of methylated sterol precursors, affects both membrane-bound proteins, including chitin synthase. The net result is an inhibition of fungal growth.⁴

Chart 1



In a program aimed at the design and synthesis of novel azole inhibitors in order to evaluate the effect of replacing the aromatic ring present in the most commonly used drugs with 1,4-benzothiazine (BT) nucleus that, in itself, shows some antifungal activity,⁵ a series of azole BT, structurally correlated with fluconazole and econazole, were recently synthesized.⁶

In the framework of this research project, we have also reported the construction of a 3D model of CYP51 of *C. albicans* (CA-CYP51) and docking experiments of a series of BT and 1,4-benzoxazine (BO) imidazole derivatives.⁷ In addition, a morphological study of the CA-CYP51 active site highlighted a hydrophobic access channel and a docking study pointed out that for all the best docking solutions the C-2 position of the BT or BO nucleus was oriented toward the access channel and the distance between C-2 and the channel entry was estimated to be about 6–7 Å. This suggested that the introduction of an alkyl chain on the nucleus base might stabilize the enzyme–drug complex by interacting with

* To whom correspondence should be addressed. Phone: +39 075 5855134. Fax: +39 075 5855161. E-mail: fringuelli@unipg.it.

[†] Department of Drug Chemistry and Technology.

[‡] Department of Experimental Medicine and Biochemical Sciences.

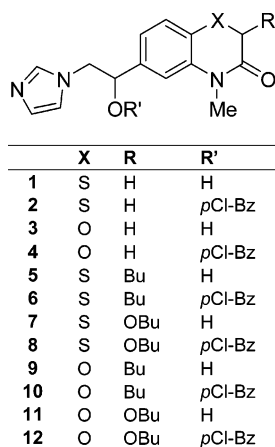


Figure 1.

the residues delimiting the channel and improve lipophilicity and fungal membrane crossing.

In the synthesis, butyl and *O*-butyl chains were introduced in C-2 of the BT and BO nuclei to furnish compounds **5–12** (Figure 1). A docking study was performed for these compounds, and results showed that the introduction of the C-2 alkyl chain really stabilizes the drug–enzyme complex and significantly improves the octanol/water partition coefficient.

Molecular Modeling

We previously reported the construction of a 3D model of CYP51 of *C. albicans* and docking experiments of a series of 1,4-BT and 1,4-BO imidazole derivatives.⁷ In particular, the CA-CYP51 model was constructed by exploiting the sequence homology relationship and the crystal structure of the CYP51 of *Mycobacterium tuberculosis* (MT-CYP51, PDB codes 1ea1, 1e9x)⁸ as template.

Although the available P450 structures show a conserved overall fold,⁹ there are variable structural features, some of which resemble protein conformational changes in response to recognition and binding of structurally diverse substrates and/or inhibitors. Thus, depending on the structural template used, these features can be exploited to construct different conformations of CA-CYP51 and aid the design of novel inhibitors.¹⁰

In our study, MT-CYP51 exhibits the P450 fold but contains structural differences that define the active site access channel. In contrast to other P450 crystal structures, the BC loop (Gly127–Leu139) adopts an open conformation in MT-CYP51. This feature gives rise to the opening of a channel (channel 1) endowed with a large mouth of about 20 Å × 10 Å that extends from the surface to the catalytic site.

Interestingly, this channel runs almost parallel to the heme in contrast to other P450 folds, such as P450BM3 and P450cam,¹¹ where another substrate access channel has been identified that runs perpendicular to the heme (channel 2). Although channel 2 is also present in MT-CYP51, it is closed by the interaction between helix A and the FG loop. Thus, channel 1 is the only substrate/inhibitor accessible pathway to the heme in the enzymatic conformation crystallized in MT-CYP51.

Constructed on the crystal structure of MT-CYP51, our model of CA-CYP51 contains the above feature that connects the surface of the enzyme to the catalytic site

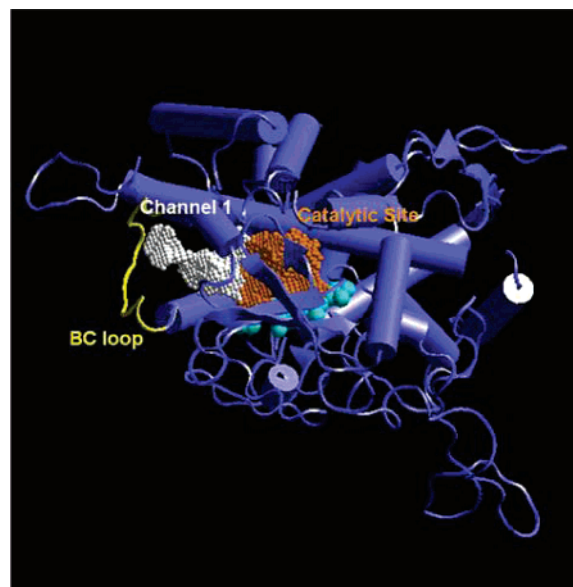


Figure 2. 3D model of CA-CYP51 used in this study. The BC loop (127–139) is highlighted in yellow. Channel 1 (white dots) extends from the surface to the catalytic site (orange dots) of heme (cyan CPK).

(Figure 2). This latter site consists of a chamber of about 1500 Å³. The dome of the chamber is 13 Å above the heme group.

The open conformation of channel 1 in the 3D model of CA-CYP51 to date has been an unexploited feature in the design of novel BT and BO imidazole inhibitors.

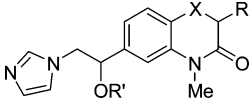
Our previous results pinpointed that BT and BO derivatives adopt similar binding modes inside the catalytic site of CA-CYP51 with subtle differences in the interactions. Furthermore, the log *P* values of these compounds strongly affect their in vitro antifungal activity with the optimal value of the water/octanol partition coefficient being >2.

On the basis of the above observations and results, we designed BT and BO derivatives with the insertion of alkyl or *O*-alkyl chains at the C-2 position of the BT and BO rings. This insertion would have the 2-fold benefit of improving the interaction energy of the inhibitors with the enzyme by filling channel 1 and increasing the log *P* value of the compounds.

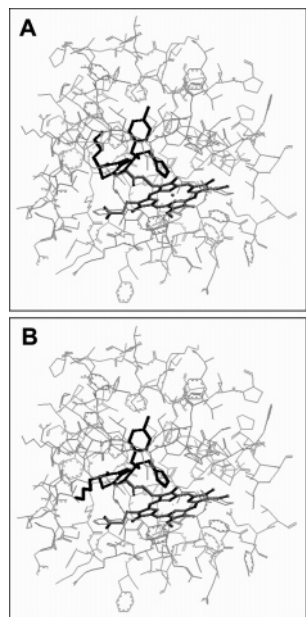
Docking experiments of each stereoisomer of compounds **5–12** were carried out in the catalytic site of CA-CYP51. Binding energies were calculated as explained in the Experimental Section and are reported in Table 1.

Although the calculated binding energies may suffer from technical (poor parametrization of the force field) and/or methodological approximations (treatment of the enzyme as a rigid body), some interesting observations can be made. Compared to their related unsubstituted analogues (**1–4**), these compounds show an improved binding energy and better log *P* values. Interestingly, the best interacting stereoisomers of compounds **5–12** show an inverted preference on the first chiral center, being shifted from 1-*S* to 1-*R*. This behavior is explained by the accommodation of the alkyl/*O*-alkyl chains into the catalytic site that forces the BT and BO rings to adopt a slightly different pose that is best fitted by the 1-*R* stereoisomers.

Table 1. Binding Energies and the log *P* Values of Different Compounds^a

compd		
	binding energy (kcal/mol)	log <i>P</i>
aS-1	-30.95 ^b	0.50
aS-2	-31.80 ^b	3.07
aS-3	-32.51 ^b	0.16
aS-4	-30.81 ^b	2.73
(a <i>R</i> ,b <i>S</i>)-5	-61.83	2.30
(a <i>R</i> ,b <i>S</i>)-6	-62.84	4.87
(a <i>R</i> ,b <i>R</i>)-7	-84.68	2.02
(a <i>R</i> ,b <i>R</i>)-8	-71.23	4.60
(a <i>R</i> ,b <i>S</i>)-9	-66.76	1.96
(a <i>R</i> ,b <i>S</i>)-10	-59.33	4.53
(a <i>R</i> ,b <i>R</i>)-11	-66.03	1.68
(a <i>R</i> ,b <i>R</i>)-12	-52.71	4.25
FLU	-29.10 ^b	1.58

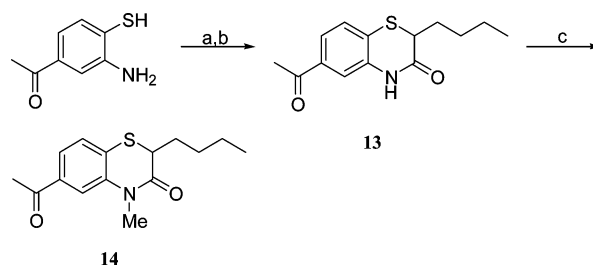
^a Only the best fitting stereoisomer is reported for each compound. ^b Data are taken from ref 7.

**Figure 3.** Binding mode of (a*R*,b*S*)-6 (A) and (a*R*,b*R*)-8 (B) into the catalytic site of CA-CYP51.

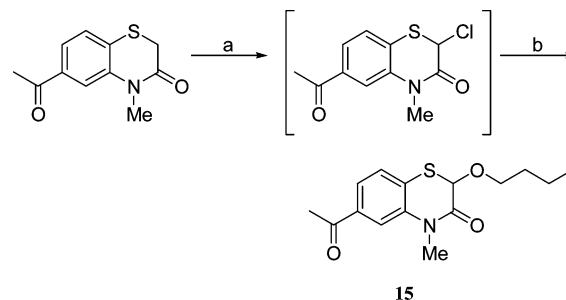
The insertion of alkyl/O-alkyl chains gives rise to a second chiral center. Depending upon the kind of substituent, the preferred configuration at the second chiral center is different in docked poses. In particular, the insertion of a butyl chain shows a 2-*S* configuration preference (Figure 3A).

In the docked pose, the butyl chain folds over the scaffold of the inhibitor and occupies the dome of the catalytic site. Conversely, upon the insertion of the one-atom-longer *O*-butyl chain, the isomer *R* shows a better binding energy. Docking experiments show that the longer chain does not fill the dome because of the presence of steric clashes but runs along channel 1 (Figure 3B).

Since the above compounds were first synthesized and tested as racemic mixtures, we cannot prove the configuration of the enantiomer. It should be mentioned, however, that neglected conformational changes of the enzyme may play a role in making room to host the substituted BT and BO rings, which in turn would favor

Scheme 1^a

^a Reagents: (a) 2-Br-hexanoic acid, 5% NaOH aqueous solution; (b) 3 N HCl; (c) *t*-BuOK, MeI.

Scheme 2^a

^a Reagents: (a) SO₂Cl₂; (b) BuOH, SiO₂.

configurations at the chiral center that are different from those predicted.

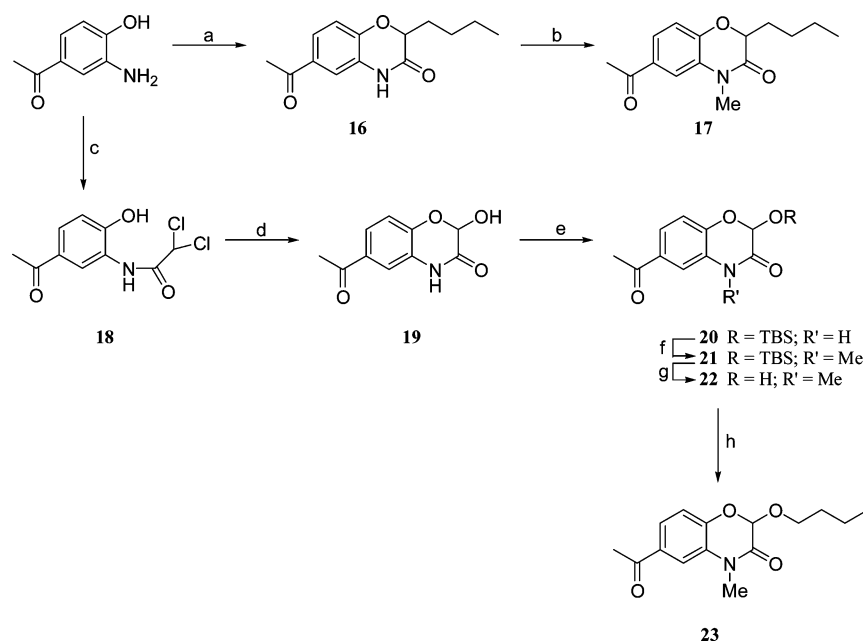
Chemistry

The intermediate 6-acetyl-2-butyl-4-methyl-3,4-dihydro-2*H*-1,4-benzothiazin-3-one (**14**) was prepared starting from 3-amino-4-mercaptoacetophenone.¹² The condensation with racemic 2-bromohexanoic acid in aqueous NaOH followed by acidification with 3 N HCl afforded **13**, which was methylated with MeI and *t*-BuOK in dry DMF to furnish **14** (Scheme 1).

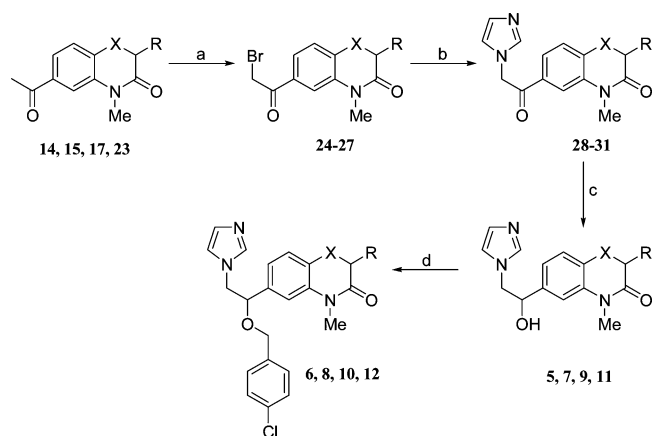
Starting from 6-acetyl-4-methyl-3,4-dihydro-2*H*-1,4-benzothiazin-3-one,¹³ 6-acetyl-2-butoxy-4-methyl-3,4-dihydro-2*H*-1,4-benzothiazin-3-one (**15**) was prepared by chlorination with sulfonyl chloride in dry benzene followed by reaction with butyl alcohol (Scheme 2).

Scheme 3 outlines the synthesis of BO intermediates **17** and **23** starting from 3-amino-4-hydroxyacetophenone.¹⁴ 2-Bromohexanoyl chloride in CHCl₃ was added dropwise to a cooled mixture of starting acetophenone, benzyltriethylammonium chloride (TEBA), and NaHCO₃ in CHCl₃. The successive methylation afforded **17**. On the other hand, 3-amino-4-hydroxyacetophenone was first reacted with dichloroacetyl chloride to give **18**, which was cyclized with NaHCO₃ to furnish **19**. The alcoholic group was protected with *tert*-butyl(dimethyl)silyl chloride (TBSCl), then methylated and deprotected under acidic conditions to afford **22**, and finally alkylated with butyl iodide to furnish the intermediate **23**.

Scheme 4 summarizes the common reactions that lead to final products **5–12** starting from key intermediates **14**, **15**, **17**, and **23**. Through the formation of bromo derivatives **24–27**, the reaction with 1*H*-imidazole supplied derivatives **28–31**, and the reduction with NaBH₄ led to carbinols **5**, **7**, **9**, and **11** that were converted into ether derivatives **6**, **8**, **10**, and **12** by reaction with *p*-chlorobenzyl chloride.

Scheme 3^a

^a Reagents: (a) NaHCO₃, TEBA, 2-Br-hexanoyl chloride; (b) NaH, MeI; (c) Cl₂CHCOCl; (d) NaHCO₃; (e) TBSCl, 1*H*-imidazole; (f) K₂CO₃, MeI; (g) 1 N HCl; (h) K₂CO₃, BuI.

Scheme 4^a

^a Reagents: (a) Br₂; (b) 1*H*-imidazole; (c) NaBH₄; (d) NaH, *p*-Cl-benzyl chloride.

Results and Discussion

In vitro anti-*Candida* activity was determined according to the NCCLS guidelines.¹⁵ Compounds were tested on *C. albicans* CA-6, clinically isolated and identified according to taxonomical criteria, and on *C. krusei* 6258, coming from the American Type Culture Collection. Results of preliminary studies are shown in Table 2. As a general consideration, introduction of the butyl chain retained or slightly improved the anti-*Candida* in vitro activity, in both the BT and BO series.

The presence of the secondary alcohol negatively affected the activity possibly because the low atom-based approach of log *P* (A log *P*) values were not influenced enough by the insertion of the alkyl chain. Alkylation of the carbinol to *p*-chlorobenzyl ether proved to be favorable, particularly with regard to anti-*C. krusei* activity.

The good in vitro activity of compounds **6** and **8** is ascribed to their strong binding energies coupled with a high lipophilic character, which allows an optimal

Table 2. In Vitro Antifungal Activities of Different Compounds^a

compd	MIC (μg/mL)	
	<i>C. albicans</i> CA-6	<i>C. krusei</i> 6258
diluent	250	250
1	125–62.5	250
2	<1.8	31.2–15.6
3	250	31.2
4	15.6–7.8	15.6
5	62.5–31.2	250
6	<1.8	<1.8
7	62.5–31.2	125
8	1.8–3.9	15.6
9	125	125
10	7.8	7.8
11	125	31.2
12	125	3.9
FLU	<1.8	62.5

^a The data represent the MIC (minimum inhibitory concentration) of various compounds against *C. albicans* or *C. krusei*. The test was performed by the microdilution method as specified in the Experimental Section.

penetration into the cytosol. The importance of the hydrophobic/hydrophilic balance is further confirmed by the poor in vitro activity of compounds **5**, **7**, **9**, and **11**. Even though these compounds are endowed with good interaction energies, an increasing hydrophilic character negatively affects their ability to cross the membrane of the fungi.

The weaker MIC of compounds **10** and **12**, which are the BO analogues of compounds **6** and **8**, is linked to their lower interaction energies.

The best compound seemed to be the BT ether derivative **6**, which showed an MIC value comparable to that of fluconazole on *C. albicans* and interesting activity on *C. krusei* (<1.8 μg/mL), partially resistant to fluconazole, on which the corresponding alcohol **5** was ineffective. The derivative that was not substituted at C-2 only had a slight activity (compare **6** with **2**).

In the BO series, the butyl chain at C-2 (**9** and **10**) did not affect the *C. albicans* inhibition profile with

Table 3. In Vivo^a Antifungal Activities of Different Compounds against *C. albicans* CA-6

	CFU ($\times 10^3$) ^b	MST ^c	range survival (day)	D/T ^d
diluent ^e	196 \pm 18	12	3–12	10/10
5	110 \pm 9	14	9–10	10/10
6	78 \pm 6	12	2 \rightarrow 30	8/10
7	143 \pm 12	14	9–10	10/10
8	127 \pm 10	14	3–17	10/10
9	230 \pm 16	14	9 \rightarrow 30	8/10
10	85 \pm 9	12	6 \rightarrow 30	8/10
11	186 \pm 10	12	4–12	10/10
12	227 \pm 19	14	8–10	10/10
FLU	0	>30	23 \rightarrow 30	2/10

^a Groups of 10 mice were inoculated iv with 1×10^5 cells of *C. albicans* CA6. Diluent, azoles, and fluconazole were given ip at a dose of 14 mg/kg, 2 h before and once daily for 8 consecutive days after infection. ^b Data represent the mean \pm SD of colony forming units (CFU) recovered from the kidneys of three mice sacrificed 11 days after infection. ^c Median survival time (days). ^d Number of dead mice at 30 days over total number of animals tested. ^e Diluent = DMSO/H₂O (1:4).

respect to the corresponding nonsubstituted compounds **3** and **4**. The alcohol derivatives were not active, while the corresponding *p*-chlorobenzyl ethers showed moderate activity. Derivative **12** showed good inhibitory activity on *C. krusei*, with an MIC value of 3.9 μ g/mL.

Since the in vitro activity did not necessarily correlate with the in vivo activity,¹⁶ the newly synthesized compounds were also tested in a murine model of systemic *C. albicans* infection. To this end, mice were treated intraperitoneally with various compounds 1 day before systemic challenge with *C. albicans* and once daily for 14 consecutive days. The results reported in Table 3 show that there is not a strict correlation between in vitro and in vivo activity for several compounds. In particular, **8** and **12**, which exhibited an antifungal effect in vitro, did not show any beneficial effect in systemic candidiasis, while a trend of correlation between anticandidal activity in vitro and beneficial effect in vivo was observed for **6** and **10**. However, despite differences in survival range, no significant difference in median survival time (MST) was observed for all groups.

It is noteworthy that an increase of survival in terms of survival range is correlated with a drastic decrease of fungal load (colony forming unit, CFU) in kidneys that represent the main target organ for *C. albicans*. This indicates that variation of dose, schedule, or route of administration could lead to optimization of the beneficial effect of different compounds on survival. In addition, another consideration emerging from these results is that compounds **5**–**12** could endow fungistatic activity in vivo, facilitating the clearance but not eradication of the fungus from the organs. This hypothesis is consistent with a significant reduction of *C. albicans* observed in the kidneys.

Conclusion

The presence of a thus far unexploited hydrophobic channel (channel 1) in the 3D model of CA-CYP 51 prompted us to design 2-substituted BT and BO. The insertion of alkyl and *O*-alkyl chains at position 2 of the BT and BO rings yielded an overall improvement of the in vitro activity. As expected, this is ascribed to both the resulting extension of the interaction surfaces

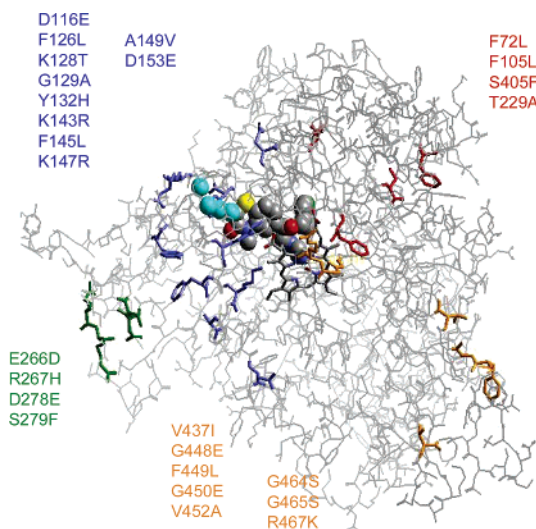


Figure 4. 3D model of CA-CYP51 in complex with (aR,bR)-**8**. Naturally occurring mutations in azole-resistant CA-CYP51 are divided into four hotspots on the basis of their structural localization. They are labeled respectively in blue, red, orange, and green. It is worth noting the proximity of the blue hotspot to the entrance of channel 1.

between the inhibitor and the enzyme channel and to the increase of the hydrophobic/hydrophilic balance. Furthermore, the presence of alkyl/*O*-alkyl substituents on the BT and BO rings allow an interesting surface region of the enzyme which is located at the mouth of channel 1 to be reached (Figure 4).

Several naturally occurring CYP51 mutations of azole-resistant *C. albicans* have been reported in this region and are clustered around the BC loop whose open/closed conformation is the gate of the above channel. The physical–chemical properties of these mutant residues can be exploited in the future to design novel BT and BO derivatives endowed with inhibitor activity toward *C. albicans* resistant strains.

Experimental Section

Melting points determined in capillary tubes (Electrothermal, model 9100, melting point apparatus) were uncorrected. Elemental analysis was performed on a Carlo Erba element analyzer 1106, and the data for C, H, and N are within $\pm 0.4\%$ of the theoretical values. ¹H NMR spectra were recorded at 200 MHz (Bruker AC-200 spectrometer) with Me₄Si as internal standard. Chemical shifts are given in ppm (δ), and the spectral data are consistent with the assigned structures. Reagents and solvents were purchased from common commercial suppliers and used as received. Column chromatography separations were carried out on Merck silica gel 60 (mesh 230–400). Yields of purified products were not optimized. Fluconazole was purchased from Pfizer (New York). All starting materials were commercially available unless otherwise indicated.

6-Acetyl-2-butyl-3,4-dihydro-2H-1,4-benzothiazin-3-one (13). 3-Amino-4-mercaptoacetophenone (18.00 g, 107.78 mmol) was suspended in 5% NaOH aqueous solution, and a mixture of 2-bromohexanoic acid (21.02 g, 107.78 mmol), NaOH (5.60 g, 140.12 mmol), and H₂O (200 mL) was added. The mixture was then heated to 70–80 °C for 20 min, then cooled at room temperature and acidified with 3 N HCl. The brown precipitate thus obtained was collected and chromatographed, eluting with CHCl₃/MeOH 98:2 to give **13** (10.21 g, 36%), mp 125–127 °C. ¹H NMR (CDCl₃) δ : 0.92 (3H, t, *J* = 7.0 Hz, CH₂CH₃), 1.25–1.75 (5H, m, SCHCHCH₂CH₂CH₃), 1.80–2.10 (1H, m, SCHCHCH₂), 2.65 (3H, s, COCH₃), 3.50

(1H, dd, $J = 8.4$ and 6.4 Hz, SCHCH₂), 7.40–7.75 (3H, m, aromatic H), 9.10 (1H, bs, CONH).

6-Acetyl-2-butyl-4-methyl-3,4-dihydro-2H-1,4-benzothiazin-3-one (14). *t*-BuOK (2.52 g, 22.57 mmol) was added to a solution of **13** (3.30 g, 12.54 mmol) in dry DMF (33 mL). The mixture was stirred at room temperature for 15 min, and then MeI (2.13 g, 15.04 mmol) in dry DMF (6 mL) was added dropwise. After being stirred for 4 h, the mixture was poured into ice-chilled water and extracted with EtOAc. The residue was chromatographed, eluting with cyclohexane/EtOAc 85:15. Compound **14** (1.04 g, 30%) was obtained as an amorphous solid. ¹H NMR (CDCl₃) δ : 0.90 (3H, t, $J = 6.9$ Hz, CH₂CH₃), 1.20–1.70 (5H, m, SCHCHCH₂CH₂CH₃), 1.75–2.00 (1H, m, SCHCHCH₂), 2.65 (3H, s, COCH₃), 3.47 (1H, dd, $J = 8.1$ and 6.4 Hz, SCHCH₂), 3.54 (3H, s, NCH₃), 7.48 (1H, d, $J = 8.0$ Hz, H-8), 7.63 (1H, dd, $J = 8.0$ and 1.6 Hz, H-7), 7.72 (1H, d, $J = 1.6$ Hz, H-5).

6-Acetyl-2-butoxy-4-methyl-3,4-dihydro-2H-1,4-benzothiazin-3-one (15). SO₂Cl₂ (0.30 g, 2.26 mmol) diluted in dry benzene (3 mL) was added dropwise over 30 min to a solution of 6-acetyl-4-methyl-3,4-dihydro-2H-1,4-benzothiazin-3-one (0.50 g, 2.26 mmol) in dry benzene (10 mL) heated to 40 °C. After being stirred at this temperature for 30 min, the mixture was gradually heated to 75 °C over 30 min, then stirred for further 30 min and evaporated to dryness. The crude residue was resuspended in dry BuOH (10 mL), and SiO₂ in a catalytic amount was added. The mixture was heated in a bain-marie for 2 h and evaporated to dryness, and the residue was chromatographed, eluting with cyclohexane/EtOAc 86:14 and thus obtaining **15** (0.38 g, 57.5%) as a white solid, mp 81–83 °C. ¹H NMR (CDCl₃) δ : 0.81 (3H, t, $J = 7.3$ Hz, CH₂CH₃), 1.10–1.20 and 1.35–1.55 (each 2H, m, CH₂CH₂CH₃), 2.66 (3H, s, COCH₃), 3.20–3.55 and 3.70–3.80 (each 1H, m, CHOCH₂), 3.60 (3H, s, NCH₃), 5.14 (1H, s, SCH₂), 7.49 (1H, d, $J = 8.0$ Hz, H-8), 7.66 (1H, dd, $J = 8.0$ and 1.5 Hz, H-7), 7.80 (1H, d, $J = 1.5$ Hz, H-5).

6-Acetyl-2-butyl-3,4-dihydro-2H-1,4-benzoxazin-3-one (16). 3-Amino-4-hydroxyacetophenone (0.50 g, 3.33 mmol) was added to a mixture of TEBA (0.75 g, 3.29 mmol), NaHCO₃ (1.13 g, 13.29 mmol), and dry CHCl₃ (18 mL), and the mixture was cooled to 0–5 °C. A solution of 2-bromoheptanoyl chloride¹⁷ (1.70 g, 7.94 mmol) in dry CHCl₃ (5 mL) was added dropwise. The mixture was heated to 55 °C and stirred for 3 h, then cooled at room temperature, stirred for 24 h, and evaporated to dryness. The crude residue was purified by chromatography, eluting with cyclohexane/EtOAc 65:35 to give **16** (0.33 g, 40%) as a white solid, mp 109–110 °C. ¹H NMR (CDCl₃) δ : 0.96 (3H, t, $J = 7.1$ Hz, CH₂CH₃), 1.25–1.70 (4H, m, CH₂CH₂CH₃), 1.75–2.10 (2H, m, CHCH₂), 2.61 (3H, s, COCH₃), 4.71 (1H, dd, $J = 8.1$ and 4.9 Hz, CHO), 7.06 (1H, d, $J = 8.4$ Hz, H-8), 7.57 (1H, d, $J = 1.9$ Hz, H-5), 7.65 (1H, dd, $J = 8.4$ and 1.9 Hz, H-7), 9.10 (1H, bs, NH).

6-Acetyl-2-butyl-4-methyl-3,4-dihydro-2H-1,4-benzoxazin-3-one (17). NaH (60% mineral oil dispersion, 0.05 g, 1.21 mmol) was added to a solution of **16** (0.20 g, 0.81 mmol) in dry DMF (2 mL). The mixture was stirred at room temperature for 30 min, and then MeI (0.17 g, 1.21 mmol) in dry DMF (1 mL) was added dropwise. After being stirred for 2 h, the mixture was poured into ice-chilled water and the precipitated was collected and chromatographed, eluting with cyclohexane/EtOAc 80:20 to furnish **17** (0.09 g, 47%) as a yellow oil. ¹H NMR (CDCl₃) δ : 0.95 (3H, t, $J = 7.0$ Hz, CH₂CH₃), 1.25–2.10 (6H, m, CH₂CH₂CH₂CH₃), 2.63 (3H, s, COCH₃), 3.45 (3H, s, NCH₃), 4.70 (1H, dd, $J = 8.2$ and 4.7 Hz, CHO), 7.07 (1H, d, $J = 8.7$ Hz, H-8), 7.60–7.75 (2H, m, H-5 and H-7).

N-(5-Acetyl-2-hydroxyphenyl)-2,2-dichloroacetamide (18). Dichloroacetyl chloride (1.07 g, 7.28 mmol) was slowly added to a solution of 3-amino-4-hydroxyacetophenone (1.10 g, 7.28 mmol) in dry THF (15 mL). After the mixture was stirred for 1 h at room temperature, a solid was filtered off. Then the solution was evaporated to dryness, and the residue was chromatographed, eluting with CHCl₃/MeOH 99:1 to give **18** (1.53 g, 80%) as a white solid, mp 196.5–197.5 °C. ¹H NMR (DMSO-*d*₆) δ : 2.51 (3H, s, COCH₃), 3.37 (1H, s, CHCl₂), 7.02

(1H, d, $J = 8.5$ Hz, H-3), 7.73 (1H, dd, $J = 8.5$ and 2.0 Hz, H-4), 8.57 (1H, d, $J = 2.0$ Hz, H-6), 10.00 (1H, bs, OH), 11.22 (1H, bs, NH).

6-Acetyl-2-hydroxy-3,4-dihydro-2H-1,4-benzoxazin-3-one (19). NaHCO₃ (0.07 g, 0.76 mmol) was added to a suspension of **18** (0.10 g, 0.38 mmol) in H₂O (4 mL). The mixture was heated to 70 °C, stirred for 2 h, then cooled to room temperature, neutralized with 3 N HCl, and extracted with EtOAc. The combined organic layers were evaporated to dryness, and the residue was purified by chromatography, eluting with CHCl₃/MeOH 96:4 to give **19** (0.06 g, 76%) as a white solid, mp 196–198 °C. ¹H NMR (DMSO-*d*₆) δ : 2.54 (3H, s, COCH₃), 5.55–5.60 (1H, m, CHOH), 7.15 (1H, d, $J = 8.3$ Hz, H-8), 7.54 (1H, d, $J = 1.0$ Hz, H-5), 7.66 (1H, dd, $J = 8.3$ and 1.0 Hz, H-7), 8.25 (1H, bs, CHOH), 11.02 (1H, s, NH).

6-Acetyl-2-([*tert*-butyl(dimethyl)silyl]oxy)-3,4-dihydro-2H-1,4-benzoxazin-3-one (20). 1H-Imidazole (0.25 g, 3.67 mmol) and TBSCl (0.43 g, 2.89 mmol) were added to a solution of **19** (0.50 g, 2.41 mmol) in dry DMF (5 mL). The mixture was stirred for 2 h at room temperature and then poured into H₂O. The precipitate was collected and purified by chromatography, eluting with cyclohexane/EtOAc 80:20 and thus obtaining **20** (0.50 g, 65%) as a white solid, mp 150 °C. ¹H NMR (CDCl₃) δ : 0.21 and 0.25 (each 3H, s, CH₃SiCH₃), 0.88 (9H, s, SiC(CH₃)₃), 2.63 (3H, s, COCH₃), 5.70 (1H, s, CHO), 7.12 (1H, d, $J = 8.4$ Hz, H-8), 7.60 (1H, d, $J = 1.8$ Hz, H-5), 7.69 (1H, dd, $J = 8.4$ and 1.8 Hz, H-7), 8.61 (1H, s, NH).

6-Acetyl-2-([*tert*-butyl(dimethyl)silyl]oxy)-4-methyl-3,4-dihydro-2H-1,4-benzoxazin-3-one (21). **20** (0.10 g, 0.31 mmol) was added to a suspension of K₂CO₃ (0.09 g, 0.65 mmol) in dry DMF (2 mL). The mixture was stirred at room temperature for 10 min, and then MeI (0.12 g, 0.37 mmol) was added. After being stirred for 3 h, the mixture was poured into ice/H₂O and the precipitated was collected. **21** (0.09 g, 90%) was obtained as a white solid, mp 82–83 °C. ¹H NMR (CDCl₃) δ : 0.19 and 0.22 (each 3H, s, CH₃SiCH₃), 0.86 (9H, s, SiC(CH₃)₃), 2.63 (3H, s, COCH₃), 3.50 (3H, s, NCH₃), 5.72 (1H, s, CHO), 7.11 (1H, d, $J = 8.0$ Hz, H-8), 7.65–7.75 (2H, m, H-5 and H-7).

6-Acetyl-2-hydroxy-4-methyl-3,4-dihydro-2H-1,4-benzoxazin-3-one (22). A solution of **21** (0.20 g, 0.60 mmol) in MeOH (10 mL) was cooled to 0–5 °C, and then 1 N HCl (2 mL) was added. The solution was stirred at room temperature for 72 h, neutralized with a saturated solution of NaHCO₃, and evaporated to dryness. The residue, chromatographed and eluting with cyclohexane/EtOAc with gradual increase of the concentration of EtOAc, furnished **22** (0.08 g, 66%) as a white solid, mp 217–220 °C. ¹H NMR (DMSO-*d*₆) δ : 2.61 (3H, s, COCH₃), 3.40 (3H, s, NCH₃), 5.70 (1H, d, $J = 5.7$ Hz, CHOH), 7.20 (1H, d, $J = 8.1$ Hz, H-8), 7.65–7.80 (2H, m, H-5 and H-7), 8.27 (1H, d, $J = 5.7$ Hz, CHOH).

6-Acetyl-2-butoxy-4-methyl-3,4-dihydro-2H-1,4-benzoxazin-3-one (23). K₂CO₃ (0.37 g, 2.71 mmol) was added to a solution of **22** (0.10 g, 0.45 mmol) in dry CH₃CN (15 mL). After the mixture was heated to 60 °C and was stirred for 15 min, BuI (0.18 g, 0.97 mmol) was added dropwise. The mixture was heated to reflux for 3 h, then evaporated to dryness, resuspended in H₂O, acidified with 3 N HCl, and extracted with EtOAc. The combined organic layers, evaporated to dryness, were chromatographed, eluting with cyclohexane/EtOAc 85:15 and thus giving **23** (0.09 g, 75%) as an amorphous solid. ¹H NMR (CDCl₃) δ : 0.87 (3H, t, $J = 7.3$ Hz, CH₂CH₃), 1.10–1.30 and 1.40–1.60 (each 2H, m, CH₂CH₂CH₃), 2.64 (3H, s, COCH₃), 3.49 (3H, s, NCH₃), 3.65–3.90 (2H, m, OCH₂), 5.49 (1H, s, CHO), 7.14 (1H, d, $J = 8.8$ Hz, H-8), 7.65–7.70 (2H, m, H-5 and H-7).

General Method for the Preparation of Bromo Derivatives 24–27. This preparation is illustrated by the synthesis of 6-(bromoacetyl)-2-butyl-4-methyl-3,4-dihydro-2H-1,4-benzothiazin-3-one (**24**).

A solution of **14** (0.80 g, 2.89 mmol) in AcOH (5 mL) was heated to 40 °C, and then Br₂ (0.55 g, 3.46 mmol) in AcOH (8 mL) was added dropwise. After being stirred for 1 h, the mixture was evaporated to dryness and the residue was

chromatographed, eluting with cyclohexane/EtOAc 94:6 to give **24** (0.47 g, 45%) as an oil. ^1H NMR (CDCl_3) δ : 0.91 (3H, t, $J = 7.2$ Hz, CH_2CH_3), 1.25–1.70 (5H, m, $\text{SCHCHHCH}_2\text{CH}_2\text{CH}_3$), 1.80–2.00 (1H, m, SCHCHHCH_2), 3.49 (1H, dd, $J = 8.1$ and 6.2 Hz, SCHCH_2), 3.55 (3H, s, NCH_3), 4.45 (2H, s, CH_2Br), 7.50 (1H, d, $J = 8.0$ Hz, H-8), 7.65 (1H, dd, $J = 8.0$ and 1.6 Hz, H-7), 7.75 (1H, d, $J = 1.6$ Hz, H-5).

General Method for the Preparation of Imidazole Derivatives 28–31. This preparation is illustrated by the synthesis of 2-butyl-6-(1*H*-1-imidazolylacetyl)-4-methyl-3,4-dihydro-2*H*-1,4-benzothiazin-3-one (**28**).

1*H*-Imidazole (0.27 g, 3.96 mmol) was added to a solution of **24** (0.47 g, 1.32 mmol) in CHCl_3 (25 mL) and stirred at room temperature for 5 h. The mixture was evaporated to dryness, and the residue was chromatographed, eluting with $\text{CHCl}_3/\text{MeOH}$ 97:3 to give **28** (0.35 g, 77%) as an amorphous solid. ^1H NMR (CDCl_3) δ : 0.91 (3H, t, $J = 6.9$ Hz, CH_2CH_3), 1.20–1.70 (5H, m, $\text{SCHCHHCH}_2\text{CH}_2\text{CH}_3$), 1.80–2.00 (1H, m, SCHCHHCH_2), 3.45–3.65 (4H, m, NCH_3 and SCHCH_2), 5.53 (2H, s, CH_2N), 7.04, 7.22 and 7.83 (each 1H, bs, imidazolic H), 7.54 (1H, d, $J = 8.0$ Hz, H-8), 7.63 (1H, dd, $J = 8.0$ and 1.3 Hz, H-7), 7.72 (1H, d, $J = 1.3$ Hz, H-5).

General Method for the Preparation of Carbinols 5, 7, 9, and 11. This preparation is illustrated by the synthesis of 2-butyl-6-[1-hydroxy-2-(1*H*-1-imidazolyl)ethyl]-4-methyl-3,4-dihydro-2*H*-1,4-benzothiazin-3-one (**5**).

NaBH_4 (0.078 g, 2.04 mmol) was added to a solution of **28** (0.35 g, 1.02 mmol) in dry MeOH (10 mL) over 1 h. The mixture was then evaporated to dryness, and the residue was chromatographed, eluting with $\text{CHCl}_3/\text{MeOH}$ 90:10 to furnish **5** (0.30 g, 85%) as an amorphous solid. ^1H NMR ($\text{DMSO}-d_6$) δ : 0.84 (3H, t, $J = 7.0$ Hz, CH_2CH_3), 1.10–1.60 (5H, m, $\text{SCHCHHCH}_2\text{CH}_2\text{CH}_3$), 1.65–1.80 (1H, m, SCHCHHCH_2), 3.33 (3H, s, NCH_3), 3.55 (1H, dd, $J = 7.7$ and 6.4 Hz, SCHCH_2), 4.00–4.30 (2H, m, CH_2N), 4.80–5.00 (1H, m, CHOH), 5.86 (1H, bs, CHOH), 6.85 and 7.48 (each 1H, s, imidazolic H), 7.00–7.25 (3H, m, aromatic H and imidazolic H), 7.37 (1H, dd, $J = 7.8$ and 1.2 Hz, H-7). Anal. ($\text{C}_{18}\text{H}_{23}\text{N}_3\text{O}_2\text{S}$) C, H, N.

General Method for the Preparation of Ether Derivatives 6, 8, 10, and 12. This preparation is illustrated by the synthesis of 2-butyl-6-[1-[(4-chlorobenzyl)oxy]-2-(1*H*-1-imidazolyl)ethyl]-4-methyl-3,4-dihydro-2*H*-1,4-benzothiazin-3-one (**6**).

NaH (60% mineral oil dispersion, 0.042 g, 1.74 mmol) was added to a solution of **5** (0.20 g, 0.58 mmol) in dry DMF (5 mL), and then *p*-chlorobenzyl chloride (0.37 g, 2.31 mmol) in dry DMF (2 mL) was added dropwise. The mixture was stirred at room temperature for 1 h, then suspended in H_2O and extracted with EtOAc. The combined organic layers were evaporated to dryness to afford a crude residue that was purified by chromatography, eluting with $\text{CHCl}_3/\text{MeOH}$ 99:1 to give **6** (0.20 g, 73%) as an oil. ^1H NMR (CDCl_3) δ : 0.91 (3H, t, $J = 7.0$ Hz, CH_2CH_3), 1.25–1.70 (5H, m, $\text{SCHCHHCH}_2\text{CH}_2\text{CH}_3$), 1.75–2.10 (1H, m, SCHCHHCH_2), 3.30–3.50 (4H, m, NCH_3 and SCHCH_2), 4.21 (2H, d, $J = 5.6$ Hz, CH_2N), 4.25 and 4.55 (each 1H, d, $J = 12.0$ Hz, CH_2Ph), 4.58 (1H, t, $J = 5.6$ Hz, CHO), 6.80–7.70 (10H, m, aromatic H and imidazolic H). Anal. ($\text{C}_{25}\text{H}_{28}\text{ClN}_3\text{O}_2\text{S}$) C, H, N.

Computational Method. The model of cytochrome P450 14 α -sterol demethylase of *Candida albicans* (CA-CYP51) was constructed using the crystal structure of cytochrome P450 of *Mycobacterium tuberculosis* (MT-CYP51, PDB codes 1ea1 and 1e9x) as previously reported by us.⁷

Azole inhibitors were built using the sketch module of Cerius-2.¹⁸ Atomic charges were calculated using the semiempirical Mopac/AM1 method. Each compound was submitted to an energy minimization protocol using the universal force field, version 1.2 software,¹⁹ and the Smart Minimizer algorithm of the Open Force Field module (OFF). Docking experiments were performed using a knowledge-based strategy.²⁰ Briefly, azole antifungals bind to MT-CYP51 through the coordination of the ring nitrogen atom (N-4 of triazole and N-3 of imidazole) to the sixth coordination position of the iron atom of the heme group. Accordingly, all compounds were manually docked in CA-CYP51 by placing the nitrogen atom in position 3 of the

imidazole ring at 2.37 Å from the heme iron along the line orthogonal to the heme plane. The value of 2.37 Å is the average distance of Fe–N coordination bonds observed in crystallized complexes of MT-CYP51 with fluconazole and 4-phenylimidazole. Starting from this docking pose, a reduced conformational profile of compounds was explored using a random sampling protocol as implemented in the Cerius-2 software package. In particular, all torsional angles of azole inhibitors, except the Fe–N coordination bond, were varied randomly in a window of $\pm 5^\circ$, generating 1000 conformations. For each enzyme–inhibitor complex, the resulting conformers were clustered on the basis of the rmsd using the autocluster protocol implemented in the conformer analysis module of Cerius-2. The center of each cluster, representing a docking solution, was submitted to a geometry optimization protocol. During the minimization, the protein was treated as a rigid body by applying fixed constraints on the coordinates of its atoms. The limitations and advantages of such a procedure were discussed in our previous work. Energy minimization was performed using the universal force field, version 1.2 software, and the Smart Minimizer protocol of the Open Force Field module (OFF). The value of the dielectric constant of the protein surrounding the binding site of the heme group was set to a value of 6.5 as reported elsewhere.²¹ Conversely, the conformational strain energy cost of the inhibitors to reach the bioactive conformation from the global minimum was determined using a dielectric constant of 80 according to the hypothesis that this process occurs in the water. The refined docking solutions were ranked according to their binding energy. For each enzyme–inhibitor complex, only the best solution, in terms of binding energy, was stored and used for further analysis. The binding energies were calculated using

$$E_{\text{bin}} = E_{\text{int}} + E_{\text{conf}} \quad (1)$$

where the energy of binding (E_{bin}) is obtained from the sum of the interaction energy (E_{int}) and the conformational strain energy (E_{conf}). The interaction energy (E_{int}) is calculated with

$$E_{\text{int}} = E_{\text{complex}} - (E_{\text{compound}} + E_{\text{protein}}) \quad (2)$$

from the docking solutions of each compound. Here, E_{complex} is the energy of the complex, E_{compound} is the energy of the docked compound, and E_{protein} is the energy of the enzyme.

The conformational strain energy (E_{conf}) is calculated as the difference between the energy of the docked conformation and the energy of the global minimum for each compound:

$$E_{\text{conf}} = E_{\text{compound}} - E_{\text{global}} \quad (3)$$

The water/octanol partition coefficient ($\log P$) was calculated using the atom-based approach (A $\log P$) as implemented in Cerius-2.²⁴ All calculations were carried out on SGI O2 R5000 and R10000 workstations.

Mycology. Mice. Female CD1 mice (8–10 weeks old, weighing 25–30 g) were obtained from Charles River Breeding Laboratories (Calco, Lecco, Italy).

C. albicans CA-6, used in this study, was isolated from a vaginal swab and identified according to the taxonomic criteria of van Uden and Buckley.²² *C. krusei* strain 6258 (American Type Culture Collection, Rockville, MD) was used in this study. The yeasts were grown at 28 °C in Sabouraud dextrose agar. Under these conditions the organisms grew as a pure yeast-phase population. Before use, yeast cells were harvested from a 24 h culture, suspended in pyrogen-free saline, washed twice, quantified by hemocytometry, and adjusted to the desired concentration.

Systemic Candidiasis Model. Mice were infected intravenously (iv) with 1×10^5 *C. albicans* blastoconidia via the lateral tail vein. Diluent (DMSO/ H_2O ratio of 1:4), chemicals, and fluconazole were administered intraperitoneally (ip) at a dose of 10 mg/kg of body weight 2 h before infection and then once daily for 14 consecutive days. The dose and administration schedules used in this study were selected from previously

reported data^{6a} and based on dose and treatment schedules reported in the literature for a novel azole with a broad antifungal spectrum, such as ER-30346.²³ For survival studies, mice were observed for 30 days. Three mice per group were killed by CO₂ asphyxiation 11 days after infection for quantitative culture of both kidneys.

Quantification of *C. albicans* in the Kidneys. The kidneys of mice were aseptically removed and homogenized with 3 mL of sterile distilled water. The number of colony forming units (CFU) was determined by a plate dilution method. Colonies of *C. albicans* cells were counted after 48 h of incubation at room temperature, and results were expressed as the number of CFU per organ.

Susceptibility Testing. Susceptibility testing was performed by the M27-A microdilution method of the National Committee for Clinical Laboratory Standards in 0.165 M MOPS (morpholinepropanesulfonic acid)-buffered (pH 7) RPMI 1640 medium (Gibco BRL, Paisley, U.K.). The activity of compounds against *C. albicans* and *C. krusei* was tested using serial dilutions ranging from 0.9 to 500 µg/mL. The MIC was the lowest concentration of chemical that produced an 80% reduction in the turbidity compared to chemical-free normal subjects.

Statistical Analysis. Differences in median survival time were determined by the Mann–Whitney U test. Student's *t* test was used to evaluate the significance of all other data. Each experiment was repeated three to five times.

Acknowledgment. This work was supported by the Italian Ministry of Education, Universities and Research, Grant COFIN 2003068044_006.

Supporting Information Available: Characterization data for compounds 7–12, 25–27, 29–31 and elemental analysis for target compounds 5–12. This material is available free of charge via the Internet at <http://pubs.acs.org>.

References

- Peres-Bota, D.; Rodriguez-Villalobos, H.; Dimopoulos, G.; Melot, C.; Vincent, J. L. Potential risk factors for infection with *Candida* spp. in critically ill patients. *Clin. Microbiol. Infect.* **2004**, *10*, 550–555.
- Sanglard, D.; Odds, F. C. Resistance of *Candida* species to antifungal agents: molecular mechanisms and clinical consequences. *Lancet Infect. Dis.* **2002**, *2*, 73–78.
- Wingard, J. R.; Leather, H. A new era of antifungal therapy. *Biol. Blood Marrow Transplant.* **2004**, *10*, 73–90.
- Lamb, D.; Kelly, D.; Kelly, S. Molecular aspects of azole antifungal action and resistance. *Drug Resist. Updates* **1999**, *2*, 390–402.
- Baruffini, A.; Pagani, G.; Amoretti, L. Derivatives of 1,4-benzothiazin-3-one. *Farmaco* **1967**, *22*, 519–528.
- (a) Fringuelli, R.; Schiaffella, F.; Bistoni, F.; Pitzurra, L.; Vecchiarelli, A. Azole derivatives of 1,4-benzothiazine as antifungal agents. *Bioorg. Med. Chem.* **1998**, *6*, 103–108. (b) Pitzurra, L.; Fringuelli, R.; Perito, S.; Schiaffella, F.; Barluzzi, R.; Bistoni, F.; Vecchiarelli, A. A new azole derivative of 1,4-benzothiazine increases the antifungal mechanisms of natural effector cells. *Antimicrob. Agents Chemother.* **1999**, *43*, 2170–2175. (c) Schiaffella, F.; Guarraci, A.; Fringuelli, R.; Pitzurra, L.; Bistoni, F.; Vecchiarelli, A. Synthesis and antifungal activity of new imidazole derivatives of 1,4-benzothiazine. *Med. Chem. Res.* **1999**, *9*, 291–305. (d) Fringuelli, R.; Pietrella, D.; Schiaffella, F.; Guarraci, A.; Perito, S.; Bistoni, F.; Vecchiarelli, A. Anti-*Candida albicans* properties of novel benzoxazine analogues. *Bioorg. Med. Chem.* **2002**, *10*, 1681–1686.
- Macchiarulo, A.; Costantino, G.; Fringuelli, D.; Vecchiarelli, A.; Schiaffella, F.; Fringuelli, R. 1,4-Benzothiazine and 1,4-benzoxazine imidazole derivatives with antifungal activity: a docking study. *Bioorg. Med. Chem.* **2002**, *10*, 3415–3423.
- Podust, L. M.; Poulos, T. L.; Waterman, M. R. Crystal structure of cytochrome P450 14 α -sterol demethylase (CYP51) from *Mycobacterium tuberculosis* in complex with azole inhibitors. *Proc. Natl. Acad. Sci. U.S.A.* **2001**, *98*, 3068–3073.
- (a) Poulos, T. L.; Finzel, B. C.; Gunsalus, I. C.; Wagner, G. C.; Kraut, J. The 2.6-Å crystal structure of *Pseudomonas putida* cytochrome P-450. *J. Biol. Chem.* **1985**, *260*, 16122–16130. (b) Ravichandran, K. G.; Boddupalli, S. S.; Hasemann, C. A.; Peterson, J. A.; Deisenhofer, J. Crystal structure of hemoprotein domain of P450BM-3, a prototype for microsomal P450's. *Science* **1993**, *261*, 731–736. (c) Poulos, T. L.; Finzel, B. C.; Howard, A. J. *J. Mol. Biol.* **1987**, *195*, 687–700. (d) Hasemann, C. A.; Ravichandran, K. G.; Peterson, J. A.; Deisenhofer, J. Crystal structure and refinement of cytochrome P450terp at 2.3 Å resolution. *J. Mol. Biol.* **1994**, *236*, 1169–1185. (e) Cupp-Vickery, J. R.; Poulos, T. L. Structure of cytochrome P450eryF involved in erythromycin biosynthesis. *Nat. Struct. Biol.* **1995**, *2*, 144–153. (f) Park, S. Y.; Shimizu, H.; Adachi, S.; Nakagawa, A.; Tanaka, I.; Nakahara, K.; Shoun, H.; Obayashi, E.; Nakamura, H.; Iizuka, T.; Shiro, Y. Crystal structure of nitric oxide reductase from denitrifying fungus *Fusarium oxysporum*. *Nat. Struct. Biol.* **1997**, *4*, 827–832. (g) Williams, P. A.; Cosme, J.; Sridhar, V.; Johnson, E. F.; McRee, D. E. Mammalian microsomal cytochrome P450 monooxygenase: structural adaptations for membrane binding and functional diversity. *Mol. Cell* **2000**, *5*, 121–131. (h) Yano, J. K.; Koo, L. S.; Schuller, D. J.; Li, H.; Ortiz de Montellano, P. R.; Poulos, T. L. Crystal structure of a thermophilic cytochrome P450 from the archaeon *Sulfolobus solfataricus*. *J. Biol. Chem.* **2000**, *275*, 31086–31092.
- (a) Sheng, C.; Zhang, W.; Zhang, M.; Song, Y.; Ji, H.; Zhu, J.; Yao, J.; Yu, J.; Yang, S.; Zhou, Y.; Zhu, J.; Lu, J. Homology modeling of lanosterol 14 α -demethylase of *Candida albicans* and *Aspergillus fumigatus* and insights into the enzyme–substrate interactions. *J. Biomol. Struct. Dyn.* **2004**, *22*, 91–99. (b) Xiao, L.; Madison, V.; Chau, A. S.; Loebenberg, D.; Palermo, R. E.; McNicholas, P. M. Three-dimensional models of wild-type and mutated forms of cytochrome P450 14 α -sterol demethylases from *Aspergillus fumigatus* and *Candida albicans* provide insights into posaconazole binding. *Antimicrob. Agents Chemother.* **2004**, *48*, 568–574. (c) Boscott, P. E.; Grant, G. H. Modeling cytochrome P450 14 α demethylase (*Candida albicans*) from P450cam. *J. Mol. Graphics* **1994**, *12*, 185–192. (d) Tsukuda, T.; Shiratori, Y.; Watanabe, M.; Ontsuka, H.; Hattori, K.; Shirai, M.; Shimma, N. Modeling, synthesis and biological activity of novel antifungal agents (1). *Bioorg. Med. Chem. Lett.* **1998**, *8*, 1819–1824. (e) Rossello, A.; Bertini, S.; Lapucci, A.; Macchia, M.; Martinelli, A.; Rapposelli, S.; Herreros, E.; Macchia, B. Synthesis, antifungal activity, and molecular modeling studies of new inverted oxime ethers of oxiconazole. *J. Med. Chem.* **2002**, *45*, 4903–4912. (f) Holtje, H. D.; Fattorusso, C. Construction of a model of the *Candida albicans* lanosterol 14- α -demethylase active site using the homology modelling technique. *Pharm. Acta Helv.* **1998**, *72*, 271–277.
- (a) Sevriokova, I. F.; Li, H.; Zhang, H.; Peterson, J. A.; Poulos, T. L. Structure of a cytochrome P450–redox partner electron-transfer complex. *Proc. Natl. Acad. Sci. U.S.A.* **1999**, *96*, 1863–1868. (b) Li, H.; Poulos, T. L. Conformational dynamics in cytochrome P450–substrate interactions. *Biochimie* **1996**, *78*, 695–699. (c) Li, H.; Poulos, T. L. The structure of the cytochrome p450BM-3 haem domain complexed with the fatty acid substrate, palmitoleic acid. *Nat. Struct. Biol.* **1997**, *4*, 140–146.
- Wada, J.; Suzuki, T.; Iwasaki, M.; Miyamatsu, H.; Ueno, S.; Shimizu, M. A new nonsteroidal antiinflammatory agent, 2-Substituted 5- or 6-benzothiazoleacetic acids and their derivatives. *J. Med. Chem.* **1973**, *16*, 930–934.
- Shridhar, D. R.; Sastri, C. V.; Bansal, O. P.; Singh, P. P.; Tripathi, R. M.; Seshagiri Rao, C.; Junnarkar, A. Y. Synthesis and pharmacology of some new oxime ethers and alkanolic acid derivatives derived from 6-acetyl-2H-1,4-benzoxazin- and -benzothiazin-3(4H)-ones. *Indian J. Med.* **1983**, *22B*, 1236–1242.
- Marc, J.; Baillarge, M. Keto derivatives of aminophenols by the Friedel–Crafts and the Fries reactions. *Bull. Soc. Chim. Fr.* **1952**, 639–642.
- Reference Method for Broth Dilution Antifungal Susceptibility Testing of Yeast; Approved Standard NCCLS Document M27-A; National Committee for Clinical Laboratory Standards: Wayne, PA, 1997.
- (a) Anaissie, E. J.; Karyotakis, N. C.; Hachem, R.; Dignani, M. C.; Rex, J. H.; Paetznick, V. Correlation between in vitro and in vivo activity of antifungal agents against *Candida* species. *J. Infect. Dis.* **1994**, *170*, 384–389. (b) Rex, J. H.; Galgiani, J. N.; Bartlett, M. S.; Espaniel-Ingroff, A.; Ghannoum, M. A.; Lancaster, M.; Odds, F. C.; Rinaldi, M. G.; Barry, A. L. Development of interpretive breakpoints for antifungal susceptibility testing: conceptual framework and analysis of in vitro–in vivo correlation data for fluconazole, itraconazole, and *Candida* infections. Subcommittee on Antifungal Susceptibility Testing of the National Committee for Clinical Laboratory Standards. *Clin. Infect. Dis.* **1997**, *24*, 235–247. (c) Rex, J. H.; Nelson, P. W.; Paetznick, V. L.; Lozano-Chiu, M.; Espinel-Ingroff, A.; Anaissie, E. J. Optimizing the correlation between results of testing in vitro and therapeutic outcome in vivo for fluconazole by testing critical isolates in a murine model of invasive candidiasis. *Antimicrob. Agents Chemother.* **1998**, *42*, 129–134.
- Ammazzalorso, A.; Amoroso, R.; Bettoni, G.; De Filippis, B. Synthesis of diastereomerically enriched 2-bromoesters and their reaction with nucleophiles. *Chirality* **2001**, *13*, 102–108.
- Cerius-2 (2001); Accelrys: San Diego, CA.

- (19) Rappe, A. K.; Casewit, C. J.; Colwell, K. S.; Goddard, W. A.; Skiff, W. M. UFF, a full periodic table force field for molecular mechanics and molecular dynamics simulations. *J. Am. Chem. Soc.* **1992**, *114*, 10024–10035.
- (20) Ji, H.; Zhang, W.; Zhou, Y.; Zhang, M.; Zhu, J.; Song, Y.; Lü, J.; Zhu, J. A three-dimensional model of lanosterol 14-demethylase of *Candida albicans* and its interaction with azole antifungals. *J. Med. Chem.* **2000**, *43*, 2493–2505.
- (21) Shimoni, E.; Tsfadia, Y.; Nachliel, E.; Gutman, M. Gaugement of the inner space of the apomyoglobin's heme binding site by a single free diffusing proton. I. Proton in the cavity. *Biophys. J.* **1993**, *64*, 472–479.
- (22) Vecchiarelli, A.; Mazzolla, R.; Farinelli, S.; Cassone, A.; Bistoni, F. Immunomodulation by *Candida albicans*: crucial role of organ colonization and chronic infection with an attenuated agerminative strain of *C. albicans* for establishment of anti-infectious protection. *J. Gen. Microbiol.* **1988**, *134*, 2583–2592.
- (23) Hata, K.; Kimura, J.; Miki, H.; Toyosawa, T.; Nakamura, T.; Katsu, K. In vitro and in vivo antifungal activities of ER-30346, a novel oral triazole with a broad antifungal spectrum. *Antimicrob. Agents Chemother.* **1996**, *40*, 2237–2242.
- (24) Viswanadhan, V. N.; Ghose, A. K.; Revankar, G. R.; Robins, R. K. Atomic physicochemical parameters for three-dimensional structure directed quantitative structure–activity relationships. 4. Additional parameters for hydrophobic and dispersive interactions and their application for an automated superposition of certain naturally occurring nucleoside antibiotics. *J. Chem. Inf. Comput. Sci.* **1989**, *29*, 163–172.

JM050685J